Modelling of Hydrogen Permeability of Structural Materials Through Protective Coating Defect

Yu. V. Zaika[*1], E. K. Kostikova[2]

[1,2]Institute of Applied Mathematical Research, Karelian Research Centre, Russian Academy of Sciences,
Pushkinskaya st. 11, Petrozavodsk, Russia 185910
[*1]zaika@krc.karelia.ru; [2]fedorova@krc.karelia.ru

***Abstract*-An efficient reduction of gaseous hydrogen isotope permeation through a metal wall is essential in several applications like hydrogen storage and distribution, hydrogen embrittlement protection, and tritium inventory in future fusion reactors like ITER. Hydrogen permeation barrier films often exhibit lower efficiency than anticipated. It is very difficult to identify and quantify the responsible mechanism since the defects can be of submicrometer dimensions and very sparsely populated. We considered hydrogen permeability through a cylindrical membrane (barrier) in the presence of protective coating defect at the inlet surface of a structural material. For various materials, when the processes of diffusion, desorption and dissolution are limiting, we present the mathematical models in the form of boundary value problems with non-linear and dynamic boundary conditions. On the basis of the implicit difference scheme, a computational algorithm of a boundary value problems solution is developed. Numerical simulation results of hydrogen permeation flux and diffusant distribution are presented. Qualitative regularities of steady state permeability regime establishment and delay times registered experimentally and depending on geometric characteristics of the membrane and physical parameters are identified.**

Keywords- Hydrogen Permeability Models; Nonlinear Boundary-value Problems; Difference Schemes; Computer Simulation

I. INTRODUCTION

The problem of hydrogen (and its isotopes) interaction with solids is a multi-faceted one [1-5]. In particular, reduction of hydrogen permeation through the protective wall of structural materials is the most important objective when solving the complex problems of hydrogen storage and transport, protection from hydrogen embitterment, and reduction of tritium content in protective systems of the future thermonuclear reactor project (ITER) monitoring. Structural material barrier provides the necessary mechanical resistance of the construction, while superimposed protective coating must block migration of hydrogen isotopes. Some areas of the structural material might be exposed to the direct effect of hydrogen and its isotopes due to defects in the protective coating. Asymptotic analysis and investigation of the geometrical factors influence on the hydrogen permeation on the surface (roughness, ruptures) and inside the membrane volume (defects of structure, interstices) has been conducted by Pisarev et al. [6]. A more detailed review (34 references) of the physical-chemical literature on this topic is provided in [7], which was the basis for the present mathematical study. The paper also considered permeation through Eurofer coated with Al and Pt coated with Al_2O_3. In [7], the model of hydrogen permeability through a cylindrical membrane (the radius of the base L, the height H) was examined, when diffusion was the only limiting process. At the inlet surface covered with a thin protective coating, there was a small radius defect in the coating ("pinhole defect") through which hydrogen permeated. The remainder of the inlet surface and the lateral surface of the cylindrical membrane were impermeable for hydrogen. Vacuum was created on the output side. At the initial time moment the membrane was dehydrogenated. Then, on the inlet side molecular hydrogen pressure increase jump-wise. If we disregard the relatively fast interjacent process, one can suppose that the concentration of dissolved hydrogen under the defect remained constant $\bar{c}$ and in equilibrium with the gaseous phase according to Sievert's law. Dissolved (atomic) hydrogen diffuses to the outlet surface, recombinates into molecules and is desorbed. Mass-spectrometer registered a permeation flux. An analytical study of the corresponding boundary value problem without accounting surface processes was carried out only for the case "an infinite plate" ($L \to +\infty$) [8, 9]. A rather detailed discussion and references are given in [7]. The main weakness of such definition of the problem is that the dynamics of surface processes which has attracted a lot of attention recently, is ignored in the model. The material sample (for example, partition of a pipeline) is assumed to be mechanically strong. The concentration of penetrating hydrogen is low due to the "pinhole defect". The linear diffusion equation is adequate for this situation and the effects of stress, strain, and deflection do not appear essential. The problem under consideration is to describe the general regularities depending on diffusion, sorption parameters (characteristics of material) and the geometric ratio. Even if the barrier retains its mechanical properties, penetration of tritium, even in small doses, can be extremely dangerous. The purpose of this study was to build a computational algorithm (in terms of difference approximation) for the simulation of hydrogen permeability for a cylindrical membrane through defective barrier coating with the account of the influence of surface processes. The results of numerical simulation provide a way, for example, to determine the limiting factors for various relations among the parameters (including geometric) and working conditions of the structural material, to estimate the value of the permeation flux and the time of its stabilization rate and to evaluate the distribution of the hydrogen concentration inside the membrane. These factors give information on the possible ways of treatment of the material (pre-training surface, various additives inside). Hydrogen isotopes are exclusively mobile, which is why experimental capabilities and the precision of measurements are significantly limited.

DOI: 10.5963/AMSA0302005

II. DIFFUSION MODEL

As a basic model of the transfer inside the membrane, the boundary-value problem of hydrogen permeability of a cylindrical sample with defect protective coating on the inlet surface was considered, when diffusion limiting factor is the only one [7-9]:

$$\frac{\partial c}{\partial t} = D\left(\frac{\partial^2 c}{\partial r^2} + \frac{1}{r}\cdot\frac{\partial c}{\partial r} + \frac{\partial^2 c}{\partial z^2}\right), \tag{1}$$

$$r \in (0, L),\ z \in (0, H),\ t \in (0, t_*),$$

$$c(t, r, 0) = c_0, \qquad r \in [0, r_0],\ r_0 < L, \tag{2}$$

$$\frac{\partial c}{\partial z}(t, r, 0) = 0, \qquad r \in (r_0, L], t \geq 0, \tag{3}$$

$$c(t, r, H) = 0, \qquad r \in [0, L],\ t \geq 0, \tag{4}$$

$$\frac{\partial c}{\partial r}(t, L, z) = 0, \qquad \frac{\partial c}{\partial r}(t + 0, z) = 0, \tag{5}$$

$$c(0, r, z) = 0, \qquad r \in [0, L],\ z \in [0, H]. \tag{6}$$

In the above equations, r_0 — radius of "pinhole defect" at the inlet surface $z = 0$, $c(t, r, z)$ — concentration of dissolved atomic hydrogen, diffusing in material; D — diffusion coefficient, $[D] = \text{cm}^2/\text{s}$. It is assumed that the experiment is carried out at a constant temperature $T = \overline{T}$, the material is nearly homogeneous, so that c_0 and D are constants. For definiteness we assume $c_0 = \bar{c} \propto \sqrt{p}$ (according to Sievert's law, the equilibrium solubility $\bar{c}$ at different inlet molecular hydrogen pressures p and temperatures T can be found in reference books). The linear dimensions of the defect are relatively small, we consider it circular and situated in the center (which is not a fundamental constraint for numerical simulation). The point of time t_* is the determined moment when the permeation flux $J(t)$ reaches the stationary value. It should be noted that the determination is asymptotic: $J(t) \approx \text{const}$, $t \geq t_*$. The point t_* should not be too large for the transition processes not to get lost against the background of the steady-flux process. The boundary condition (2) corresponds to the rapid (in the scale of t_*) establishment of local equilibrium on the inlet side. The condition $\partial_r c(t, +0, z) = 0$ follows from the spatial symmetry of $c(t, r, z)$.

The aim is to develop the algorithm of numerical simulation of the flux of hydrogen from the outlet surface of a cylindrical membrane. For the purpose of this model (1)–(6):

$$J(t) = -D\int_0^L \frac{\partial c}{\partial z}\Big|_{z=H} 2\pi r\, dr.$$

The counting is done in atoms ($[J] = 1/\text{s}$), although it is the hydrogen molecules that are registered. Atomic desorption becomes significant only at very high temperatures. Change in the formulation of $J(t)$ and the overall model including the process of recombination of H atoms to the molecule on the surface (in the near-surface bulk) are described in the next sections.

Modelling makes it possible to reveal diffusion kinetics specificity and to estimate the significance of sizes membrane and defect ratios. It is possible to analyze the spatial distribution of H in the sample at any time. In the first approximation there is one physical parameter — the diffusion coefficient D, which "bifurcates" to preexponential factor D_0 and activation energy of E_D due to the temperature dependence according to the law of Arrhenius $D(T) = D_0 \exp\{-E_D/[RT]\}$.

Remark. Formally initial zero data (6) do not agree with the initial condition (2) when $t = +0$ (instant jump of concentration). From the mathematical point of view, the solution to a boundary value problem should be considered within the theory of generalized solutions. A realistic quick transition process (during the first few steps of the experiment t) was taken into account when the model was discretized and numerical simulation was conducted. The jump can be considered a formal notation of this initial stage, in this case all models can be considered as a compact "continuous" representation of a discrete process.

III. NUMERICAL APPROACH: DIFFERENCE APPROXIMATION

We consider the diffusion model (1)–(6) as a base for further development to take into account the dynamics of surface processes, therefore its presentation will be done in detail, then we will point out necessary modifications.

Following a standard technique [10], the grid in space is introduced

$$\Omega_h = \left\{(r_i, z_j)\Big|_{z_j = jh_z, 0 \leq j \leq N_2, h_z = H/N_2}^{r_i = ih_r,\ 0 \leq i \leq N_1, h_r = L/N_1}\right\},$$

and the grid at the time $\omega_\tau = \{t_k = k\tau, 0 \leq k \leq K, \tau = t_*/K\}$. The value of $r_0 = 0$ and radius of defect $r_0 \in (0, L)$ differ according to the context. Let us denote approximate values of the inside concentration of $c(t_k, r_i, z_j)$ by $c_{i,j}^k$. To make the presentation easier during the transition from k-th to $(k+1)$-th layer at time t if the number of the layer is left out:

DOI: 10.5963/AMSA0302005

$$c_{i,j} = c_{i,j}^{k}, \bar{c}_{i,j} = c_{i,j}^{k+1/2}, \hat{c}_{i,j} = c_{i,j}^{k+1}, \quad (r_i, z_j) \in \Omega_h.$$

The implicit scheme of alternating direction is considered for Eq. (1). The scheme is called a longitudinal-transverse or Peaceman-Rachford scheme [10]. The transition from k-th to $(k+1)$-th layer is carried out in two stages. At the first stage the intermediate values of $\bar{c}_{i,j}$ are determined from ratios

$$\frac{\bar{c}_{i,j} - c_{i,j}}{0,5\,\tau D} = \frac{c_{i,j-1} - 2\,c_{i,j} + c_{i,j+1}}{h_z^2} + \frac{\bar{c}_{i-1,j} - 2\,\bar{c}_{i,j} + \bar{c}_{i+1,j}}{h_r^2} + \frac{\bar{c}_{i+1,j} - \bar{c}_{i-1,j}}{2\,r_i h_r}.$$

At the second stage, using the already known $\bar{c}_{i,j}$, we find $\hat{c}_{i,j}$ of

$$\frac{\hat{c}_{i,j} - \bar{c}_{i,j}}{0,5\,\tau D} = \frac{\hat{c}_{i,j-1} - 2\,\hat{c}_{i,j} + \hat{c}_{i,j+1}}{h_z^2} + \frac{\bar{c}_{i-1,j} - 2\,\bar{c}_{i,j} + \bar{c}_{i+1,j}}{h_r^2} + \frac{\bar{c}_{i+1,j} - \bar{c}_{i-1,j}}{2\,r_i h_r}. \quad (7)$$

Approximation data (for the first and second stages) are considered in the internal nodes of the grid ($i = 1, \ldots, N_1 - 1$, $j = 1, \ldots, N_2 - 1$). Approximation accuracy is $O(\tau^2 + h_r^2 + h_z^2)$. For $r \to 0$ ($h_r \to 0$) due to the condition $\partial_r c|_{+0} = 0$ and taking into account $\partial_r c / r \approx \partial_r^2 c$ for the nodes with the number $i = 1$ we use difference approximation of the equation $\partial_t c = D[2\partial_r^2 c + \partial_z^2 c]$.

A. Radius r Sweeping

The transition from k-th to $(k+1/2)$-th layer is considered. In the notation

$$A_i = \frac{1 - [2i]^{-1}}{\varkappa}, \quad B_i = \frac{1 + [2i]^{-1}}{\varkappa} \quad \left(i = \frac{r_i}{h_r}\right), \quad \varkappa = 2\left[1 + \frac{h_r^2}{D\tau}\right],$$

$$F_{i,j} = (h_r h_z^{-1})^2 \varkappa^{-1}[c_{i,j-1} - 2c_{i,j} + c_{i,j+1}] + [1 - 2\varkappa^{-1}]c_{i,j} \quad (k \geq 0)$$

for every fixed $j = 1,2, \ldots, N_2 - 1$ we obtain

$$A_i \bar{c}_{i-1,j} - \bar{c}_{i,j} + B_i \bar{c}_{i+1,j} + F_{i,j} = 0 \quad (0 < i < N_1). \quad (8)$$

The values at the initial moment of time $t = 0$ (the zero layer) are known: $c_{i,j}^0 = 0$. Following the sweep method [10], we seek the approximate concentration values in the grid nodes on the $(k+1/2)$-th layer ($k \geq 0$) in the form of

$$\bar{c}_{i,j} = \alpha_{i+1,j}\,\bar{c}_{i+1,j} + \beta_{i+1,j} \quad (0 \leq i < N_1). \quad (9)$$

The sweep coefficients ($i = 2,3, \ldots, N_1$) are:

$$\alpha_{i,j} = \frac{B_{i-1}}{1 - A_{i-1}\,\alpha_{i-1,j}}, \quad \beta_{i,j} = \frac{F_{i-1,j} + A_{i-1}\,\beta_{i-1,j}}{1 - A_{i-1}\alpha_{i-1,j}}. \quad (10)$$

Let's specify the initial coefficients.

- The ratio of (8) for $i = 1$ is:

$$\frac{1}{2\varkappa}\,\bar{c}_{0,j} - \bar{c}_{1,j} + \frac{3}{2\varkappa}\,\bar{c}_{2,j} + F_{1,j} = 0. \quad (11)$$

  From the boundary condition (5) ($\partial_r c|_{+0} = 0$) with an accuracy $O(h_r^3)$ we have (here and further formulae of numerical differentiation of the form $f_0' \approx [-3f_0 + 4f_1 - f_2]/[2h]$, $f_2' \approx [f_0 - 4f_1 + 3f_2]/[2h]$ are used)

$$0 = 2h_r \partial_r c(t_{k+1/2}, +0, z_j) \approx -\bar{c}_{2,j} + 4\bar{c}_{1,j} - 3\bar{c}_{0,j}. \quad (12)$$

  Taking into account (11) and (12), we find $\alpha_{1,j} = (6 - \varkappa)/4$, $\beta_{1,j} = F_{1,j}\varkappa/4$.

- If $r \to +0$ we have $\partial_r c / r = (\partial_r c(t,r,z) - \partial_r c(t,+0,z))/r \approx \partial_r^2 c$. The initial coefficients of $\alpha_{1,j}$, $\beta_{1,j}$ are found from the approximation of the equation $\partial_t c = D(2\partial_r^2 c + \partial_z^2 c)$ on the $(k+1/2)$-th layer at $i = 1$ (Eq. (1) is approximated for $i > 1$) and conditions $\partial_r c|_{+0} = 0$:

$$2(\bar{c}_{0,j} + \bar{c}_{2,j})\varkappa^{-1} - \bar{c}_{1,j}(1 + 2\varkappa^{-1}) + F_{1,j} = 0, \ \bar{c}_{2,j} = 4\bar{c}_{1,j} - 3\bar{c}_{0,j}, \quad (13)$$

  due to $\alpha_{1,j} = (6 - \varkappa)/4$, $\beta_{1,j} = F_{1,j}\varkappa/4$. The forms are similar.

- Axial symmetry of concentration distribution is used for the location of the first sweep coefficients. The value of the $r = 0$ corresponds to the axis of the cylinder. Spatial area $[0, L] \times [0, H]$ can be regarded as half of the axial cross-section of the cylinder. Formally a symmetrical node ($i = -1$) is added then letting

$$\bar{c}_{-1,j} = \bar{c}_{1,j} \quad (\bar{c}_{-1,j} \approx c(t_{k+1/2}, -h_r, z_j) = c(t_{k+1/2}, h_r, z_j)).$$

  Continuing to operate formally, let us write down the Eq. (8) for $i = 0$ ($r \approx 0$), taking into account the condition of symmetry:

$$\frac{\bar{c}_{-1,j}}{\varkappa}\left(1 - \frac{h_r}{2r}\right) - \bar{c}_{0,j} + \frac{\bar{c}_{1,j}}{\varkappa}\left(1 + \frac{h_r}{2r}\right) + F_{0,j} = 0, \quad \bar{c}_{-1,j} = \bar{c}_{1,j}.$$

DOI: 10.5963/AMSA0302005

With the exception (division by $r \approx 0$) if the condition $\bar{c}_{-1,j} = \bar{c}_{1,j}$ "is reduced", we get $\alpha_{1,j} = 2/\varkappa$, $\beta_{1,j} = F_{0,j}$. Note that when $h_r^2/[D\tau] \approx 1$, $h_r \ll 1$ ($c_{0,j} \approx c_{1,j}$) we have $\varkappa \approx 4$, $F_{0,j} \approx F_{1,j}$ and almost the same value of $\alpha_{1,j}$, $\beta_{1,j}$. It is expedient to adhere to the comparability of $h_r^2/[D\tau] \sim 1$ to be able to compare the accuracy of the derivatives approximation by time and spatial variables.

- Function continuation is symmetrical: $c(t,r,z) = c(t,-r,z)$ ($r < 0$), that is $r \in [-L, L]$. The diffusion equation is the same. Tractable exception $\partial_t c = D(2\partial_r^2 + \partial_z^2 c)$, $r = \pm 0$ is due to $\partial_r c|_{+0} = 0$ for $r = 0$. Formally, we "stick together" the diffusion equation on $[-L, L]$. Similarly, we obtain the ratio of (13) as $2(\bar{c}_{-1,j} + \bar{c}_{1,j})/\varkappa - \bar{c}_{0,j}(1 + 2/\varkappa) + F_{0,j} = 0$. Assuming $\bar{c}_{-1,j} = \bar{c}_{1,j}$, we find $\alpha_{1,j} = 4/(2+\varkappa)$, $\beta_{1,j} = F_{0,j}\varkappa/(2+\varkappa)$.

Numerical experiments showed that the considered variants of primary sweep coefficients determination when calculation is executed on a rather fine grid, leading to virtually the same results.

After the forward sweep pass has been executed (coefficients $\alpha_{i,j}$, $\beta_{i,j}$ have been determined) *the nearest aim* to determine the value $\bar{c}_{N_1,j}$, is required for backward sweep. Writing approximation of the first boundary conditions from (5) taking into account $r = L$ ($\partial_r c(t, L, z) = 0$), we have

$$2h_r \partial_r c(t_{k+1/2}, L, z_j) \approx \bar{c}_{N_1-2,j} - 4\bar{c}_{N_1-1,j} + 3\bar{c}_{N_1,j},$$

in the boundary node with an accuracy $O(h_r^3)$. We substituted expressions for $\bar{c}_{N_1-2,J}$, $\bar{c}_{N_1-1,j}$ in formula (9) and determined that

$$\bar{c}_{N_1,j} = \frac{\beta_{N_1,j}(4 - \alpha_{N_1-1,j}) - \beta_{N_1-1,j}}{3 + \alpha_{N_1,j}(\alpha_{N_1-1,j} - 4)}, \quad 0 < j < \mathrm{N}_2.$$

By formula (9), the values $\bar{c}_{i,j}$ ($0 \le i < N_1$, $0 < j < N_2$) are calculated.

Now we find missing values $\bar{c}_{i,j}$ for $j = 0$ and $j = N_2$, $0 \le i \le N_1$. We have $\bar{c}_{i,N_2,} = 0$ taking into account boundary condition (4) when $z = H$ ($c(t, r, H) = 0$). Let's denote $i_0 = \max\{i : r_i \le r_0\}$, then we obtain $\bar{c}_{i,0} = c_0$ ($0 \le i \le i_0$) and $\bar{c}_{i,0} = (4\bar{c}_{i,1} - \bar{c}_{i,2})/3$ ($i_0 < i \le N_1$) from the boundary conditions (2), (3) (at $z = 0$).

B. z Variable Sweeping

The transition from the $(k + 1/2)$-th to the $(k + 1)$-th layer is executed in two steps, because cylindrical coordinates have an exception at $r \to +0$ and on the boundary $z = 0$ we have a mixed boundary condition.

The first step: $i = 1$, $r \to +0$ ($h_r \ll r_0$, $\partial_r c/r \approx \partial_r^2 c$), the sweeping algorithm is carried out for the diffusion equation $\partial_t c = D(2\partial_r^2 c + \partial_z^2 c)$. Its approximation is:

$$\frac{\hat{c}_{1,j} - \bar{c}_{1,j}}{0,5\,\tau D} = \frac{\hat{c}_{1,j-1} - 2\,\hat{c}_{1,j} + \hat{c}_{1,j+1}}{h_z^2} + 2\,\frac{\bar{c}_{0,j} - 2\,\bar{c}_{1,j} + \bar{c}_{2,j}}{h_r^2} \ (0 < j < N_2).$$

In the notations $G = 2(1 + h_z^2/[D\tau])$, $\bar{F}_{1,j} = 2(h_z h_r^{-1})^2(\bar{c}_{0,j} - 2\bar{c}_{1,j} + \bar{c}_{2,j}) + (G - 2)\bar{c}_{1,j}$, we obtain

$$\hat{c}_{1,j-1} - G\,\hat{c}_{1,j} + \hat{c}_{1,j+1} + \bar{F}_{1,j} = 0, \quad k \ge 0. \tag{14}$$

We seek approximate values of the concentration on the (k + 1)-th layer in the form

$$\hat{c}_{1,j} = \alpha_{1,j+1}\,\hat{c}_{1,j+1} + \beta_{1,j+1}, \quad 0 \le j < N_2, k \ge 0. \tag{15}$$

We seek sweeping coefficients ($1 < j \le N_2$), substituting formula $\hat{c}_{1,j-1} = \alpha_{1,j}\hat{c}_{1,j} + \beta_{1,j}$ ($0 < j < N_2$) in (14):

$$\alpha_{1,j} = \frac{1}{G - \alpha_{1,j-1}}, \ \beta_{1,j} = \frac{\bar{F}_{1,j-1} + \beta_{1,j-1}}{G - \alpha_{1,j-1}}. \tag{16}$$

Initial sweeping coefficients $\alpha_{1,1}, \beta_{1,1}$ are found taking into account formula (15) when $j = 0$ and conditions (2) ($\hat{c}_{1,0} = c_0$): $\alpha_{1,1} = 0$, $\beta_{1,1} = c_0$.

The second step: We have $i = 2, \ldots, N_1 - 1$, $r > 0$ and execute the sweep method for the Eq. (1). We obtain

$$\hat{c}_{i,j-1} - G\hat{c}_{i,j} + \hat{c}_{i,j+1} + \bar{F}_{i,j} = 0, \quad k \ge 0, \tag{17}$$

for differential formula (7) using the notation

$$\bar{F}_{i,j} = \left(\frac{h_z}{h_r}\right)^2 \left[\left(1 - \frac{1}{2i}\right)\bar{c}_{i-1,j} - 2\left(1 - \frac{h_r^2}{D\tau}\right)\bar{c}_{i,j} + \left(1 + \frac{1}{2i}\right)\bar{c}_{i+1,j}\right].$$

We seek concentration values in the grid nodes at the $(k + 1)$-th layer in the form

$$\hat{c}_{i,j} = \alpha_{i,j+1}\,\hat{c}_{i,j+1} + \beta_{i,j+1}, \quad 0 \le j < N_2, k \ge 0. \tag{18}$$

DOI: 10.5963/AMSA0302005

Sweep coefficients ($j = 2, \dots, N_2$) are:

$$\alpha_{i,j} = \frac{1}{G - \alpha_{i,j-1}}, \quad \beta_{i,j} = \frac{\bar{F}_{i,j-1} + \beta_{i,j-1}}{G - \alpha_{i,j-1}}. \tag{19}$$

We find initial sweep coefficients for $r \le r_0$ ($i \le i_0$) from (18) for $j = 0$, taking into account conditions (2) $\hat{c}_{i,0} = c_0$: $\alpha_{i,1} = 0$, $\beta_{i,1} = c_0$. Initial coefficients for $r > r_0$ ($i > i_0$) are determined with (17) for $j = 1$, taking into account the boundary conditions (3) $\partial_z c(t, r, 0) = 0$, $r > r_0$ ($-3\hat{c}_{i,0} + 4\hat{c}_{i,1} - \hat{c}_{i,2} = 0$): $\alpha_{i,1} = 2 - G/2$, $\beta_{i,1} = \bar{F}_{i,1}/2$.

Boundary values are obtained from the conditions (4): $\hat{c}_{i,N_2} = 0$ ($0 \le i \le N_1$). These values are necessary for backward sweep method executing. We compute $\hat{c}_{i,j}$ ($0 < i < N_1$, $0 \le j < N_2$), assuming formulae (15), (18).

We find missing approximate concentration values $\hat{c}_{i,j}$ for $i = 0$ and $i = N_1$, $0 \le j < N_2$. We obtain $\hat{c}_{0,j} = (4\hat{c}_{1,j} - \hat{c}_{2,j})/3$, from boundary conditions (5) ($\partial_r c|_{+0} = 0$) and approximation (12). Similarly, we have $\hat{c}_{N_1,j} = (4\hat{c}_{N_1-1,j} - \hat{c}_{N_1-2,j})/3$, according to the first condition in (5) $\partial_r c(t, L, z) = 0$.

We may propose another method for computing using an additional (fictitious) node, similar to r radius sweeping section. Then, the boundary concentration values (for $i = 0$) will be searched during z variable sweep, and values $\bar{F}_{0,j}$ will be determined, formally assuming, that we will have nodes $\hat{c}_{-1,j}$ ($\hat{c}_{-1,j} = \hat{c}_{1,j}$).

The criterion of hydrogen balance control is used for calculation errors monitoring:

$$\int_0^{t_*} [-D \int_0^{r_0} \partial_z c|_0 \, 2\pi r \, dr] dt - \int_0^{t_*} [-D \int_0^{L} \partial_z c|_H \, 2\pi r \, dr] dt = \int_0^{H} \int_0^{L} c\,(t_*, r, z)\, 2\pi r \, dr dz \equiv Q.$$

There is the difference between the number of hydrogen atoms dissolved in the membrane on the inlet surface through defect of a coating and the number of hydrogen atoms that left the membrane from the outlet surface is in the left side of the formula, the number of hydrogen inside the membrane is in the right side of the formula. Technically, other checking time points could be taken instead of t_*. The input and outward fluxes can be denoted by

$$J_0(t) \equiv -D \int_0^{r_0} \partial_z c(t, r, 0)\, 2\pi r \, dr, \quad J_H(t) \equiv -D \int_0^{L} \partial_z c(t, r, H)\, 2\pi r \, dr.$$

We monitor disbalance (relating to "measurements in outlet") at the 1 percent level in software support:

$$\frac{\int_0^{t_*} J_0(t)\, dt - \int_0^{t_*} J_H(t)\, dt - Q}{\int_0^{t_*} J_H(t)\, dt} \le 0.01.$$

Richardson extrapolation was used to improve the accuracy of the calculations $C(t, r, z) = (4c_{h_r/2}(t, r, z) - c_{h_r}(t, r, z))/3$ (see [11] for example). The method of a grid condensation (adaptive grid [12]) was used for experiments with radius of defect $r_0 \ll L$.

IV. NUMERICAL SIMULATION

A. Dimensionless Form of the Boundary-value Problem

To present the results of numerical simulation we pass to dimensionless variables, using values intrinsic for this problem: $u = c/c_0$, $\rho = r/L$, $\zeta = z/H$, $\tau = (D/L^2)t$. The value of L^2/D is treated as the characteristic time of the concentration stabilization due to diffusion. In the areas with length-scale parameters comparable to L (on vertical direction, z-direction) diffusion is faster for $H \sim L$, due to vacuum from the outlet side). Denoting the additional $\rho_0 = r_0/L < 1$, $R = L/H$, we get a dimensionless boundary-value problem:

$$\begin{aligned}
&\frac{\partial u}{\partial \tau} = \frac{1}{\rho}\frac{\partial}{\partial \rho}\left(\rho \frac{\partial u}{\partial \rho}\right) + R^2 \frac{\partial^2 u}{\partial \zeta^2}, \quad \rho, \zeta \in (0,1),\\
&u(\tau, \rho, 0) = 1, \qquad \rho \in [0, \rho_0], \tau > 0,\\
&\frac{\partial u}{\partial \zeta}(\tau, \rho, 0) = 0, \qquad \rho \in (\rho_0, 1], \tau \ge 0,\\
&u(\tau, \rho, 1) = 0, \qquad \rho \in [0,1], \tau \ge 0,\\
&\frac{\partial u}{\partial \rho}(\tau, 1, \zeta) = 0, \qquad \frac{\partial u}{\partial \rho}(\tau, +0, \zeta) = 0,\\
&u(0, \rho, \zeta) = 0, \qquad \rho \in [0,1],\ \zeta \in [0,1].
\end{aligned}$$

Varying parameters are $R > 0$ and $\rho_0 \in (0,1)$. Formally, we obtained a diffusion equation in anisotropic environment: $D_\rho = 1$, $D_\zeta = R^2$. The smaller H (the thinner the membrane) is, the faster the diffusion in the ζ-direction (on the z axis). Coefficient D_ζ

DOI: 10.5963/AMSA0302005

represents the ratio of the cylindrical membrane geometric characteristics. During the "time" τ the significant "length" in ρ direction is $\sqrt{\tau}$, and in ζ direction is $R\sqrt{\tau}$. Steady-state ($\partial_\tau u \approx 0$) is determined by the value $\tau_* = (D/L^2)t_*$.

Let us introduce a dimensionless, average (on the base of the π square) outward flux

$$U(\tau) = -\frac{1}{\pi}\int_0^1 R^2 \frac{\partial u}{\partial \zeta}\Big|_{\zeta=1} 2\pi\rho\, d\rho.$$

The function $U(\tau)$ increases monotonically approaching asymptotically a steady-state value $U_* = U(\tau_*)$. If a protective coating is absent (formally consider $\rho_0 = 1$), we have a maximum of $U_* = R^2$ ($\partial_\rho u = 0$, $\partial_\zeta u|_{\tau_*} = -1$).

The original averaged flux can be represented by

$$I(t) \equiv \frac{J(t)}{\pi L^2} = \frac{Dc_0}{H} V(\tau)\ (\tau = DL^{-2}t), \quad V(\tau) \equiv R^{-2}U(\tau) = -2\int_0^1 \frac{\partial u}{\partial \zeta}\Big|_{\zeta=1} \rho\, d\rho.$$

The value of Dc_0/H is the permeation steady-state flux density for a membrane without protective coating ($\rho_0 = 1$). Consequently, the number $V(DL^{-2}t) \in (0,1)$ is a fraction of $I(t)$ in the highest possible density of the output flux Dc_0/H. Letting $\rho_0 = 1$ we have a maximum $V_* = 1$.

To be specific, the range for the diffusion coefficient is fixed as $D: 10^{-8} - 10^{-5}$ cm$^2/s$. We will consider cylindrical membrane dimension as comparable with a coin (the barrier of a local industrial pipeline). We'll focus on these parameters values: $\rho_0 = \{1/50, 2/50, \ldots, 1/5\}$, $R = \{1/3, 1/2, 7/10, 1, 3/2, 3, 5, 7, 10\}$.

There is little doubt that the coating is actually protective for larger values of ρ_0. During the initial steps at the time when the amount of dissolved hydrogen inside the membrane is small to negligible, but the hydrogen concentration in the near-surface bulk under coating defect has already reached $u(\rho, 0) = 1$ ($\rho \le \rho_0$), there is a jump-like concentration discontinuity in the nodes near the defect. Hydrogen concentration under the defect of protective coating increases gradually but relatively quickly to smooth this initial dramatic increase when we solve this dimensionless problem. It corresponds to the physical estimates and is only formalized in the model by the initial hydrogen concentration sudden change. Numerical experiment is carried out with a small step $\Delta\tau$ (Δt of the order of seconds — during this time, nothing noticeable will happen in the "coin"). Defining $u(\Delta\tau, \rho, 0) = 10^{-3}$, $u(2\Delta\tau, \rho, 0) = 10^{-2}$, $u(3\Delta\tau, \rho, 0) = 10^{-1}$, $u(4\Delta\tau, \rho, 0) = 1/2$, and $u(5\Delta\tau, \rho, 0) = 1$, $\rho \le \rho_0$, during five steps we reach the level of $u = 1$ under the defect. Formally, the start time point of the experiment is shifted for monitoring hydrogen balance: $0 \to 5\Delta\tau$.

Output parameters of the computing experiment are the values of τ_*, τ_0, U_* (V_*), where τ_0 is the delay time, calculated by

$$\tau_0 = \tau_* - S(\tau_*)[\dot{S}(\tau_*)]^{-1} = \tau_* - S(\tau_*)U^{-1}(\tau_*), \quad S(\tau) \equiv \int_0^\tau U(\tau)\, d\tau$$

($\dot{S} \equiv dS/d\tau$). In the original time we obtain $t_0 = t_* - \int_0^{t_*} J(t)dt/J(t_*)$. Geometrically this is the point of intersection of the axis t with asymptotes of the graph of the function $Q(t) = \int_0^t J(\tau)d\tau$ (the number of permeating through membrane of hydrogen atoms). The accuracy of calculation of $\tau_0(t_0)$ increases with increasing $\tau_*(t_*)$ taking into account the asymptotic behavior of the stabilized mode permeation flux. The time of permeation flux stabilization, the value of the steady-state flux and the delay time are experimentally registered data. These values serve as the input information for the inverse problem of kinetic parameters estimation of hydrogen permeability by measurements (see, e.g. [13, 14] ($\rho_0 = 1$)). In this paper, the direct problem is solved, to reveal qualitative dependencies of these values on parameters of the model.

B. Criteria of Stop and Their Testing

The following two conditions are used for a criterion of stop:

$$\{U(\tau_n) > \alpha(\rho_0 R)^2\} \wedge \{[U(\tau_n) - U(\tau_{n-\tilde{n}})]R^{-2} < \varepsilon\}.$$

Here the first condition is necessary to exclude stopping at the beginning of the experiment, when the output flux is very small. The reference values are the max $U_* = R^2$ ($\rho_0 = 1$) and proportionality of U_* in linear approximation of the defect square ($\propto \rho_0^2$). The coefficient α is an empirical one, we used the value $\alpha = 1/30$ for fixing the range of model parameters. The second condition is triggered when the flux change is relatively insufficient during detectable time of a real experiment (for example, $t_n - t_{n-\tilde{n}} \approx 10$ min.). Another possible criterion of stop is: $\{\ddot{U}(\tau_n) < 0\} \wedge \{[U(\tau_n) - U(\tau_{n-\tilde{n}})]/[CR^2] < \varepsilon\}$. In this case, the first condition takes into account the fact that the flux graphics have a flex point: the curve is convex at the beginning of the experiment, and it becomes concave approaching steady state.

Numerical experiments were carried out for a variety of C: $C_1 = \rho_0^2$ (in Fig. 1 stop moments for different ε are denoted ○), $C_2 = U(\tau_{n-\tilde{n}})$ (■ in Fig. 1), $C_3 = \tau_n - \tau_{n-\tilde{n}}$ (△ in Fig. 1). The results of variation of R and ρ_0 showed that condition for the limitation of the output flux "derivative" works better (△). For the following calculations we used values $C = C_3$ and $\varepsilon = 10^{-3}$.

DOI: 10.5963/AMSA0302005

Additionally, calculation checking was carried out for $\rho_0 = 1$, and his case corresponds to a membrane without a protective coating. Investigation of hydrogen permeability of a stationary plate allows analytic solution for the considered model. Calculations confirmed that concentration is $u(\tau, \rho, \zeta) = 1 - \zeta$ $(\tau \geq \tau_*)$ and the delay time through the plate of thickness ℓ is equal to $\ell^2/[6D]$ [1], and it is $1/[6R^2]$ under our notation. In addition, we checked asymptotic $U_* \to R^2$ for $\rho_0 \to 1$.

C. Discussion of Computer Simulation

Figs. 2-8 present the results of numerical simulation with for different values of R and ρ_0. The results of a computational experiment in dimensionless form are three main characteristics: τ_*, τ_0, U_* $(V_* = R^{-2}U_*)$. By default, the sequence of the recording of values corresponds to descending maximums. The curve for $R = 1.5$ is indicated by a dotted line. "Interfluve value" $R = 1.5$ is rather nominal. It should suggest relatively small and large R at a qualitative level. Translation to the original variables is defined by values D, L. Weak dependence of dimensionless characteristics τ_*, τ_0 on the radius of the defect is observed in Figs. 2 and 3. We restrict the discussion to the case of $\rho_0 < 0.2$, because this is the adopted border when coating is really protective. Extremum of functions $\tau_*(\rho_0)$, $\tau_0(\rho_0)$ is observed for $R < 1.5$ (derivative sign changes, in Figs. 4 and 5). This is caused by the growing influence of the boundary conditions (insulated lateral surface). Functions $\tau_*(\rho_0)$, $\tau_0(\rho_0)$ for $R \geq 1.5$ are monotonic. The rate of stationary value change U_* for variation of R and ρ_0 can be estimated in Figs. 6 and 8.

At a qualitative level, we obtained the following results focusing on an "ideal" experimental error under 10% and not distinguishing output model fluxes under 1%. The influence of the boundary conditions with $r = L$ on stationary permeation flux is insignificant for $R = L/H > 3$, $\rho_0 < 0.2$, this membrane may be considered as a plate $(L \to +\infty)$ (see Fig. 8). This corresponds to the findings in [7, 9]. Consequently, analytical methods of research are useable for $R > 3$. Practically, it is possible to estimate when permeation flux is proportional to the number of defects (their density). In addition, the developed software allows to analyze spatial distribution of hydrogen in the membrane at any points of time (Figs. 9 and 10).

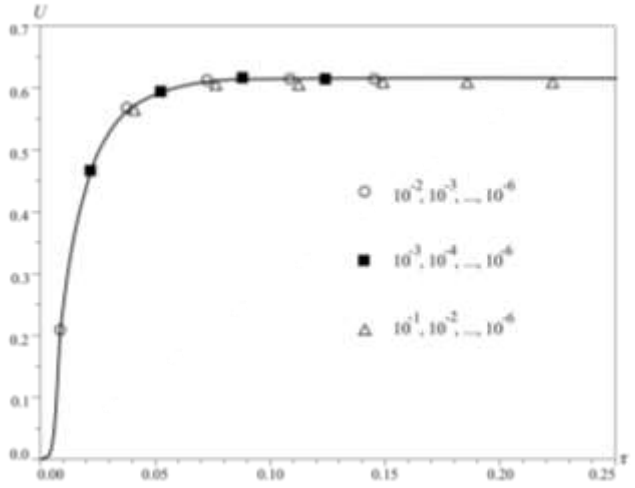

Fig. 1 Criterion of stop: $R = 5$, $\rho_0 = 0.08$ $(D = 10^{-7})$

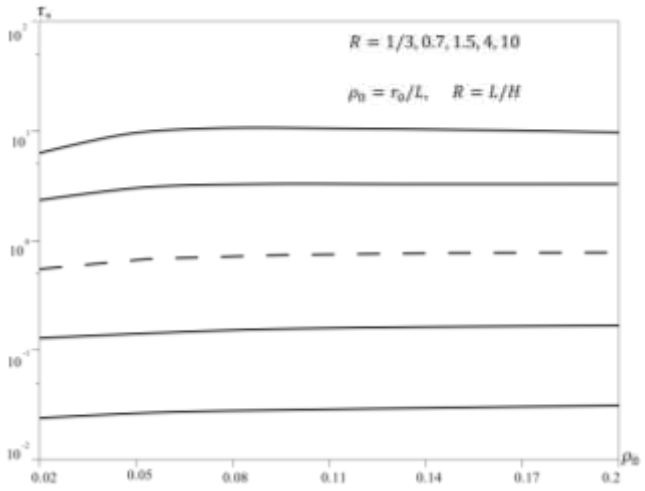

Fig. 2 Flux stabilization time

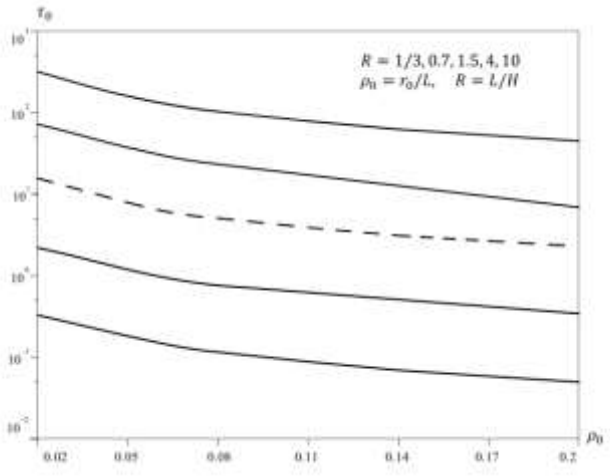

Fig. 3 Delay time

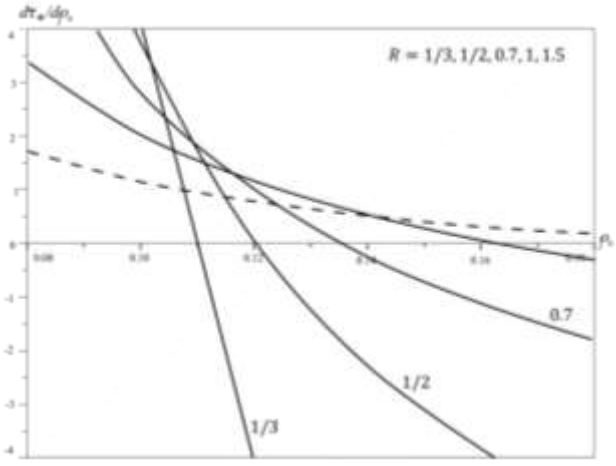

Fig. 4 Rate of τ_* change $(R \leq 1.5)$

DOI: 10.5963/AMSA0302005

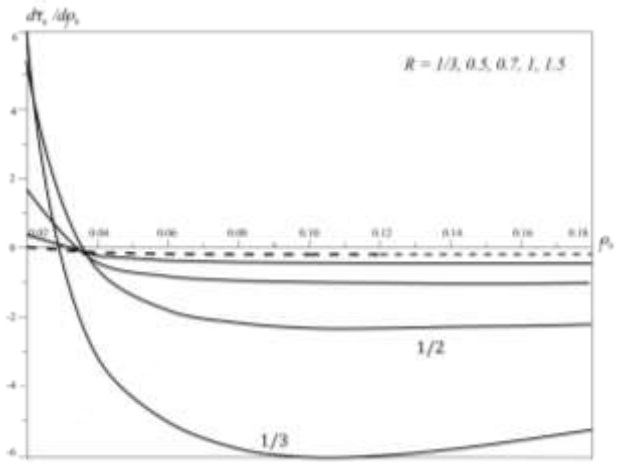

Fig. 5 Rate of τ_0 change ($R \leq 1.5$)

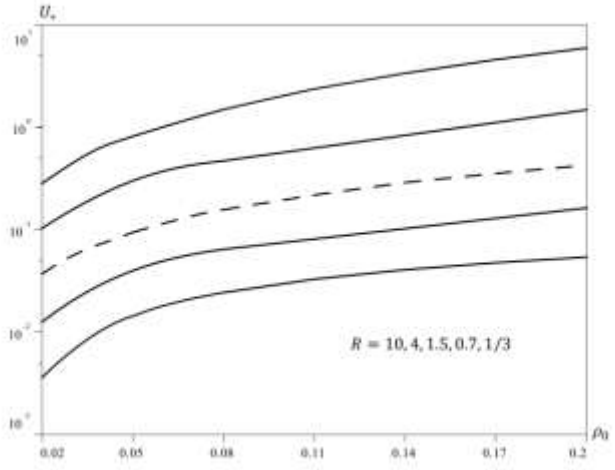

Fig. 6 Stabilization U value

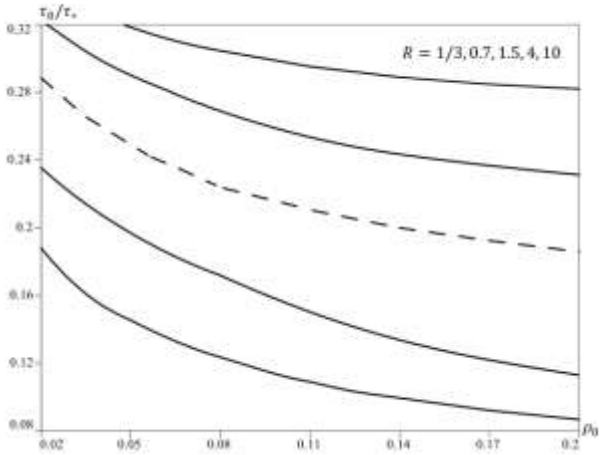

Fig. 7 Delay time fraction vs experimental time

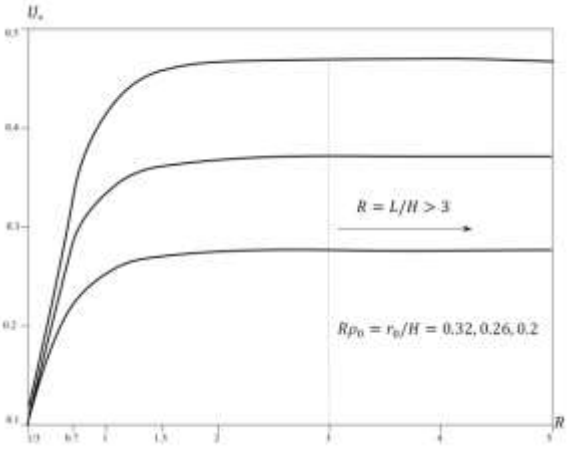

Fig. 8 Steady state permeation flux, $R\rho_0 = \text{const}$

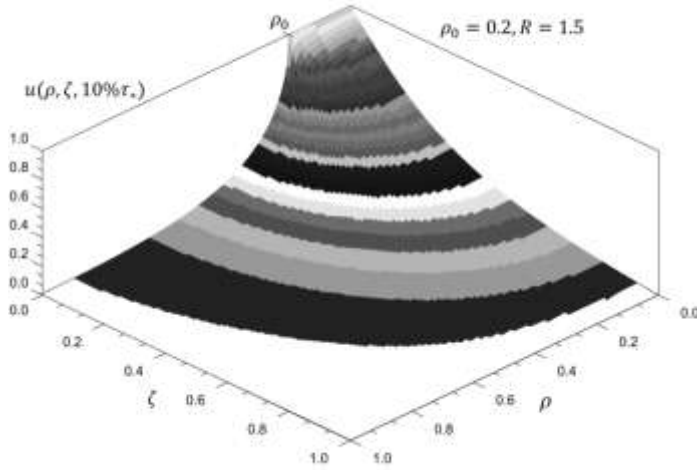

Fig. 9 Concentration profile for $\tau = 0.1\tau_*$

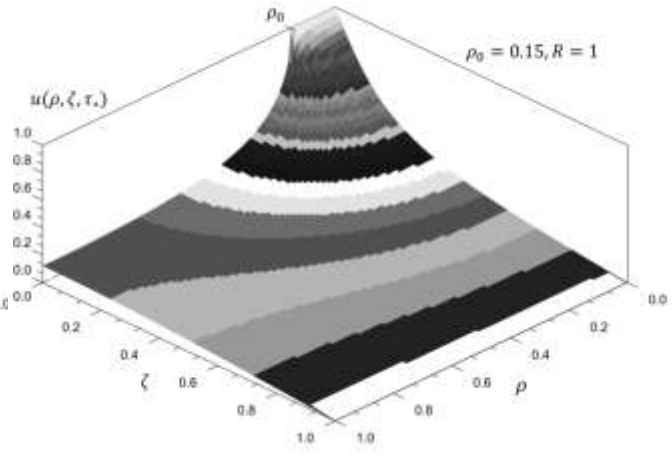

Fig. 10 Steady-state concentration level: $\rho_0 = 0.15$, $R = 1$

DOI: 10.5963/AMSA0302005

V. MODEL WITH BULK DESORPTION

Now, we focus on the model that takes into account the dynamics of surface processes. We shall not consider a multistage process of hydrogen permeability in detail, due to limited amount of experimental information. We consider only integral parameters. The boundary conditions (2), (4) are substituted by the following

$$\mu sp - bc^2(t,r,0) = -D\left.\frac{\partial c}{\partial z}\right|_{z=0},\ r \in [0,r_0], \tag{20}$$

$$bc^2(t,r,H) = -D\left.\frac{\partial c}{\partial z}\right|_{z=H},\ r \in [0,L], \tag{21}$$

$$J(t) = \int_0^L b\,c^2(t,r,H)\,2\pi r\,dr.$$

In the above equations, b is a coefficient of bulk desorption (effective recombination [6, 15]), μ is a kinetic constant, p is the molecular hydrogen pressure, and s is a coefficient of hydrogen adhesion to the surface. Within the scope of a gas kinetic theory, μp is particles flux density (in this case, molecule) encountering with the surface. Only a small number of hydrogen atoms ("incident" particles in the form of H_2 molecules) dissolve inside the membrane ($s \ll 1$). Formally, the coefficient s generally presents the multistage process including adsorption, dissociation of H_2 molecules to atoms and dissolution. In the context of inverse problems of model parametric identification it is possible to go into detail, if necessary. Additionally, the inlet and outlet surfaces may have different properties, they are easily taken into account in the course of modelling: $b = b_1$ at $z = 0$ and $b = b_2$ at $z = H$ (see asymptotics in [16]). The hydrid phases development and disintegration are more difficult to be taken into account (see [17]), if these processes are important. In the paper we focus on relatively homogeneous materials. Vacuum is created at the outlet of the membrane, so resorption (item $\mu s_2 p_2$) in (21) is ignored. Output desorption flux is counted by atoms ($[J] = 1/\mathrm{c}$). In equilibrium state the condition (20) ($\partial_z c = 0$) becomes $\mu \mathrm{sp} = b\bar{c}^2$, that is Sievert's law.

The boundary conditions (20), (21) should be read as flux balance: μsp is the input hydrogen atoms flux density; bc^2 is the desorption density (generalized process, which includes the output of atoms on the surface and their recombination to molecules); and $-D\partial_z c$ are the densities of the diffusion inward and outward fluxes. Let the temperature be constant, it is technically easy to modify the computational algorithm in terms of $T = T(t)$, using Arrhenius dependencies on, for example, $D(T) = D_0 \exp\{-E_D/[RT]\}$ (R is absolute gas constant, E is activation energy). It is assumed that the heating is rather slow to consider it uniform when Fick's law remains valid with modification $D = D(t) \equiv D(T(t))$. Kinetic constant μ weakly depends on temperature ($\mu \propto 1/\sqrt{T}$), this dependence may be formally included in $s(T)$. The value is used in numerical experiments $\mu = 1.46 \cdot 10^{21}\ \mathrm{cm^{-2}s^{-1}Torr^{-1}}$.

Numerical simulation makes it possible to estimate how fast the defect concentration under protective coating is stabilized in scale duration time t_* (outward flux stabilization), and how the concentration $c(t_*, r, 0)$ differs from the equilibrium concentration level $\bar{c}$. In addition, information about sensitivity of $J(t)$ to variations in diffusion coefficient and surface processes ("derivatives" on D, b, s) is of special interest.

We will now explain the basic algorithm modifications.

A. Counter-Sweep Method

Consider the transition from the $(k+1/2)$-th to the $(k+1)$-th layer, sophistication of the algorithm is caused mainly by finding the boundary concentrations $c_{i,0}$ ($i \le i_0$), c_{i,N_2}. Differential ratio inside the membrane remains the same. We will search approximate values of concentration for three point difference Eqs. (14), (17), in the following form ($1 \le i \le i_0$, $k \ge 0$):

$$\hat{c}_{i,j} = \alpha_{i,j+1}\hat{c}_{i,j+1} + \beta_{i,j+1} + \gamma_{i,j+1}\hat{c}_{i,0}, \quad 0 \le j < N_2;$$

$$\hat{c}_{i,j} = \hat{\alpha}_{i,j-1}\hat{c}_{i,j-1} + \hat{\beta}_{i,j-1} + \hat{\gamma}_{i,j-1}\hat{c}_{i,N_2},\ 0 < j \le N_2,$$

focusing on the idea of the counter-sweep method [10]. The sweep coefficients are

$$\alpha_{i,j+1} = (G - \alpha_{i,j})^{-1}, \hat{\alpha}_{i,j-1} = \alpha_{i,N_2-(j-1)},$$

$$\beta_{i,j+1} = (\beta_{i,j} + \bar{F}_{i,j})\alpha_{i,j+1}, \hat{\beta}_{i,j-1} = (\hat{\beta}_{i,j} + \bar{F}_{i,j})\hat{\alpha}_{i,j-1},$$

$$\gamma_{i,j+1} = \gamma_{i,j}\alpha_{i,j+1}, \hat{\gamma}_{i,j-1} = \gamma_{i,N_2-(j-1)}.$$

The benefit of this variation of a sweep method is in fact that initial sweep coefficients are readily determined $\alpha_{i,1} = \beta_{i,1} = \hat{\beta}_{i,N_2-1} = 0$, $\gamma_{i,1} = 1$. In the notations $\Delta = \alpha_{i,N_2-1} - 4$,

$$\mathbb{A} = 3 + \alpha_{i,N_2}\Delta,\ \mathbb{B} = \beta_{i,N_2-1} + \beta_{i,N_2}\Delta,$$

DOI: 10.5963/AMSA0302005

$$\widehat{\mathbb{B}} = \hat{\beta}_{i,1} + \hat{\beta}_{i,0}\Delta, \quad \mathbb{G} = \gamma_{i,N_2-1} + \gamma_{i,N_2}\Delta$$

we obtain the approximation of conditions (20), (21) with an accuracy up to $O(h_z^2)$:

$$\begin{cases} 2h_z D^{-1} b\, \hat{c}_{i,0}^2 + \mathbb{A}\hat{c}_{i,0} + \mathbb{G}\hat{c}_{i,N_2} + \widehat{\mathbb{B}} - 2h_z D^{-1}\mu sp = 0, \\ 2h_z D^{-1} b\, \hat{c}_{i,N_2}^2 + \mathbb{A}\hat{c}_{i,N_2} + \mathbb{G}\hat{c}_{i,0} + \mathbb{B} = 0. \end{cases}$$

The system of equations has a unique solution $\hat{c}_{i,0} > 0$, $\hat{c}_{i,N_2} > 0$, at any rate for small $h_r \sim h_z$ (comparable by the order).

We have to obtain the values of $\hat{c}_{i,j}$ for $i = 0$, $i > i_0$, $0 \le j \le N_2$. The changes will affect the boundary $z = H$. The differential Eq. (17) is executed inside the membrane as before. Sweeping coefficients are determined by (19) as in the diffusion model above. Modification appears after running the forward sweep pass. We approximate (21) with accuracy to $O(h_z^2)$ ($f'_2 \approx [f_0 - 4f_1 + 3f_2]/[2h]$) and use (18) to find $\hat{c}_{i,N_2}$:

$$2h_z bD^{-1}\hat{c}_{i,N_2}^2 + \mathbb{A}\hat{c}_{i,N_2} + \mathbb{B} = 0, \quad i_0 < i < N_1.$$

Quadratic equation roots have different signs at small $h_r \sim h_z$. Physically, the root is chosen positive. Then we determine values $\hat{c}_{i,j}$ ($i = 0$ and $i = N_1$, $0 \le j \le N_2$) according to conditions $\partial_r c|_{0,L} = 0$ (approximations on the three-point stencil).

During the transition from the k-th to the $(k + 1/2)$-th layer on t the boundary values of $\bar{c}_{i,0}$, $\bar{c}_{i,N_2}$ ($0 \le i \le N_1$) are calculated as the positive roots of the quadratic equation obtained after substitution in (20), (21) approximations

$$\partial_z \bar{c}|_{z=0} \approx \frac{-\bar{c}_{i,2} + 4\bar{c}_{i,1} - 3\bar{c}_{i,0}}{2h_z}, \quad \partial_z \bar{c}|_H \approx \frac{\bar{c}_{i,N_2-2} - 4\bar{c}_{i,N_2-1} + 3\bar{c}_{i,N_2}}{2h_z}, \tag{22}$$

where $\bar{c}_{i,1}$, $\bar{c}_{i,2}$, $\bar{c}_{i,N_2-1}$, $\bar{c}_{i,N_2-2}$ are known from the results of r radius sweep. The values of $\bar{c}_{i,j}$ ($0 < j < N_2$) are obtained from the relations specified above. Inside the membrane and on boundaries $r = 0$, $r = L$, everything remains as in the base model.

B. Iterative Method

The derivative is approximated by $\partial_z c(t_{k+1}, r, 0) \approx [-3\hat{c}_{i,0} + 4\hat{c}_{i,1} - \hat{c}_{i,2}]/[2h_z]$ on the $(k + 1)$-th layer taken with respect to time. Substituting $z = 0$ in the boundary condition (20), we find $\hat{c}_{i,0} = f_0(\hat{c}_{i,1}, \hat{c}_{i,2})$ as a positive root of the quadratic equation. Similarly, concentrations $\hat{c}_{i,N_2} = f_{N_2}(\hat{c}_{i,N_2-1}, \hat{c}_{i,N_2-2})$ are defined as a positive root of the quadratic equation, approximating the condition (21) ($z = H$). Values $\hat{c}_{i,1}$, $\hat{c}_{i,2}$, $\hat{c}_{i,N_2-1}$, $\hat{c}_{i,N_2-2}$ are preliminarily calculated by an explicit difference scheme approximating the equation of diffusion (1). We used a standard explicit two-layer four-pointed stencil [2]. With the current $\hat{c}_{i,0}$, $\hat{c}_{i,N_2}$, we solve the tridiagonal system of linear algebraic equations using the sweep method on the z-variable direction, and we find new concentrations approximation $\hat{c}_{i,1}$, $\hat{c}_{i,2}$, $\hat{c}_{i,N_2-1}$, $\hat{c}_{i,N_2-2}$ (and other values of $\hat{c}_{i,j}$ for $j = 3, \dots, N_2 - 3$, $i = 0, \dots, i_0$). We solve quadratic equations relative to $\hat{c}_{i,0}$, $\hat{c}_{i,N_2}$ again and repeat the calculations as long as the boundary values are stabilized (usually 2–3 iterations are enough). Finding approximations of $\hat{c}_{i,j}$ for $i > i_0$ is described above. Then we move to the next layer taken with respect to time.

C. Discussion of Simulation Results

Let us pass to dimensionless variables: $u = \frac{c}{c_0}$, $\rho = \frac{r}{L}$, $\zeta = \frac{z}{H}$, $\tau = \frac{D}{L^2}t$, $R = \frac{L}{H}$, $\rho_0 = \frac{r_0}{L}$. Concentration c_0, $c_0 < \bar{c}$ for $\rho_0 = 1$ can be taken as a normalizing concentration. However, we accept $c_0 = \bar{c}$ ($u \le 1$), having the extensive "equilibrium" reference information about metals and alloys available. For the purpose of the model we have $\bar{c} = \sqrt{\mu sp/b}$. Conditions (20), (21) can be written in the form

$$\hat{p}\hat{b}u^2(\tau, \rho, 0) = -\left.\frac{\partial u}{\partial \zeta}\right|_{\zeta=0}, \quad \rho \in [0, \rho_0], \tag{23}$$

$$\hat{b}u^2(\tau, \rho, 1) = -\left.\frac{\partial u}{\partial \zeta}\right|_{\zeta=1}, \quad \rho \in [0,1], \tag{24}$$

$$\hat{b} \equiv \frac{bc_0 H}{D}, \quad \hat{p} \equiv \hat{\mu} sp, \quad \hat{\mu} \equiv \frac{\mu H}{Dc_0}, \quad c_0 = \bar{c}.$$

The pressure p of molecular hydrogen on the input surface is constant. The coefficient $\hat{b}$ is equal to the ratio of $b\bar{c}^2$ (local desorption density when concentration is close to equilibrium $\bar{c}$) to $D\bar{c}/H$ (density of permeation flux in the diffusion regime, when $c|_H = 0$, $\rho_0 = 1$, $t \ge t_*$). Meanwhile, the outlet flux (μsp) is normalized by value $D\bar{c}/H$. For equilibrium state we have $\mu sp = b\bar{c}^2$, hence $\hat{b} = \hat{p}$. We denote this parametric variable $\hat{b}$ by W. We obtain in the present model

DOI: 10.5963/AMSA0302005

$$W = HbD^{-1}S\sqrt{p}\ (H\sqrt{p}FD^{-1} = L\sqrt{p}F[RD]^{-1}),$$

where $F \equiv \sqrt{b\mu s}$, $S \equiv \sqrt{\mu s/b}$ is dissolution ($\bar{c} = S\sqrt{p}$).

W is called a transporting parameter when protective coating is absent ($\rho_0 = 1$) [6]: if $W \gg 1$ diffusion limits permeation (diffusion limited regime — DLR), and the asymptotic condition $W \ll 1$ corresponds to the SLR (surface limited regime). The transitory area is estimated within $W \in (10^{-2}, 10^4)$. For the problem under consideration when hydrogen permeates through a defect of the protective coating ($\rho_0 < 1$) we have three independent parameters R, ρ_0, and W. The value of R^2 serves as a "diffusion coefficient" in the ζ direction, and W parametrizes the left parts of the boundary conditions (23), (24): $u \in (0,1)$, $W[1 - u^2(\tau, \rho, 0)]$, $Wu^2(\tau, \rho, 1)$.

Formally, hydrogen adsorption by the membrane stops at $u = 1$. Concentration c is less than equilibrium concentration $\bar{c}$ due to vacuum: resorption is ignored at the boundary condition (24). Inward "diffusion" flux $R^2\partial_\zeta u$ ($z = 0$) can be significant for $u \approx 1$ and $R^2\partial_\zeta u \approx 0$, due to $R \gg 1$. For fixed value of R (excluding variants $R \ll 1$ / $R \gg 1$ when permeability is practically non-existent or the plate is infinite) asymptotic accordance of $W \to 0$, $W \to +\infty$ to regimes SLR, DLR is valid. It should be noted that small W value (due to $bs \ll 1$) may correspond to large dissolution value ($S \propto \sqrt{s/b}$).

To be specific, we focus on the following parameter ranges for numerical simulation: $p \in [0.1,10]$ Torr, $H \in [0.01,0.5]$ cm, $D \in [10^{-8}, 10^{-5}]$ cm^{2}s^{-1}, $s \in [10^{-8}, 10^{-3}]$, $b \in [10^{-25}, 10^{-14}]$ cm^{4}s^{-1} $\left(L = RH,\ \bar{c} = \sqrt{\mu s p b^{-1}}\right)$.

We obtain in terms of dimensionless variables

$$J(t) = \int_0^L bc^2(t, r, H)\, 2\pi r\, dr = \frac{D\bar{c}}{H}\, \pi L^2 V(\tau), \quad V(\tau) \equiv 2\int_0^1 \hat{b}u^2(\tau, \rho, 1)\rho\, d\rho.$$

The value V formally means the permeation flux fraction of $D\bar{c}H^{-1}\pi L^2$ (stationary flux value in case of the protective coating absence ($r_0 = L$) and $c = \bar{c}$ ($z = 0$), $= 0$ ($z = H$)).

Input parameters are R, ρ_0, $\hat{b}$ for the dimensionless problem. As a criterion of stop we assume the following condition

$$\{\ddot{V}(\tau_n) < 0\} \wedge \{X^{-1}[V(\tau_n) - V(\tau_{n-\bar{n}})][\tau_n - \tau_{n-\bar{n}}]^{-1} < \varepsilon\}.$$

Here the value $\tau_n - \tau_{n-\bar{n}}$ corresponds to the order of 10 minutes of real experimental time t, $\varepsilon = 10^{-3}$. For the problem with bulk desorption the standardizing value $V_*|_{\rho_0=1}$ is equal to X, which is the solution to the equation $(\sqrt{\hat{p} - X} - \hat{b}^{1/2}X)^2 = X$. Indeed, this formula is obtained from boundary conditions (23) and (24) for $\rho_0 = 1$, assuming time derivative equals to zero in the diffusion equation. Here variable $X = -\partial_\zeta u$ ($\tau = \tau_*$) is equal to $\max V(\tau_*) = V_*$ ($\rho_0 = 1$). In more detail, we find the value of normalization X in the following way. Stationary distribution is linear: $u_*(\zeta) = A\zeta + B$ ($\partial_t u = 0$, $\partial_\rho u = 0 \Rightarrow \partial_z^2 = 0$) for $\rho_0 = 1$. We obtain $V_* = -\partial_\zeta u_* = -A$, using (24) and the definition of $V(\tau)$. The boundary conditions for $\rho_0 = 1$, $\tau \geq \tau_*$ give $\hat{p} - \hat{b}B^2 = V_*$, $\hat{b}[-V_* + B]^2 = V_*$. Excluding B, we obtain the equation $(\sqrt{\hat{p}V_*} - \hat{b}^{1/2}V_*)^2 = V_*$. This equation has the only solution $V_* = X \in (0,1)$ ($B = u_*(0) < 1$, $u_*(1) > 0 \Rightarrow V_* = -A < B < 1$).

Now we pass to the results of computational experiments. The difference scheme was presented in physical terms, but the scheme (not only experimental results) can be rewritten in the adopted dimensionless units. Figs. 11 and 12 show the influence of the membrane geometric characteristics (defect and membrane sizes) on the experimental output parameters. The sequence of values listing corresponds to the descending maximums in presented figures. In our numerical simulation we used the following values of parameters: $b = 10^{-24}$ cm^4/s, $H = 0.1$ cm, $D = 10^{-6}$ cm^2/s, $s = 10^{-8}$, $p = 10$ Torr. Here we have $t = L^2D^{-1}\tau = R^2H^2D^{-1}\tau \Rightarrow \tau = t/[10^4R^2]$.

DOI: 10.5963/AMSA0302005

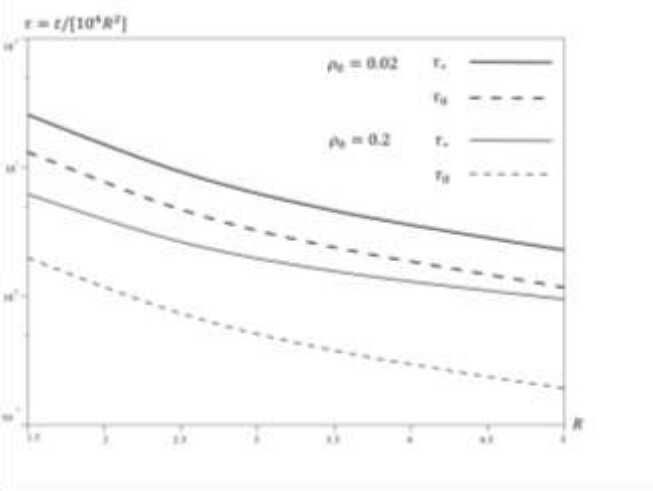

Fig. 11 Stabilization and delay times

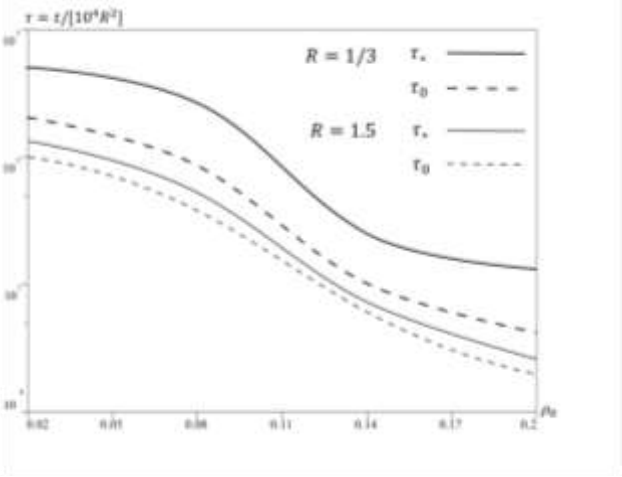

Fig. 12 Steady state permeation flux, $R\rho_0 = \text{const}$

VI. MODEL WITH SURFACE DESORPTION

Boundary conditions (2), (4) substitute the following

$$\frac{\partial q_0}{\partial t} = \mu sp - bq_0^2(t,r) + D\frac{\partial c}{\partial z}\Big|_0, \quad r \in [0, r_0], \tag{25}$$

$$\frac{\partial q_H}{\partial t} = -bq_H^2(t,r)D\frac{\partial c}{\partial z}\Big|_{z=H}, \quad r \in [0, L], \tag{26}$$

$$c(t,r,0) = gq_0(t,r), \quad c(t,r,H) = gq_H(t,r),$$

$$q_0 = q_H = 0 \ (t = 0), \quad J(t) = \int_0^L bq_H^2(t,r)\, 2\pi r\, dr.$$

Here q_0, q_H are the surface concentrations on the inlet and outlet surfaces, $[q] = 1/\text{cm}^2$; g is a coefficient of concordance between the hydrogen atoms concentration in the near-surface bulk and on the surface (a coefficient of fast dissolution, $[g] = 1/\text{cm}$); and b is a coefficient of surface desorption, $[b] = \text{cm}^2/\text{c}$. The diffusion and desorption parameters dependence on temperature T we consider by law of Arrenius are $D = D_0 \exp\{-E_D/[RT]\}$, $b = b_0 \exp\{-E_b/[RT]\}$. Other dependences on T are assumed, if necessary. Temperature dependence of the variable μ is formally taken into account in the coefficient $s(T)$. It is not important in what follows because the temperature is constant during the experiment performed by the permeability method.

The meaning of s (without getting involved in the details) is the following: μsp is the hydrogen atoms flux density where mobile atoms are trapped on the surface. Boundary conditions (25), (26) mean adsorption, desorption and diffusion flux disbalance is due to hydrogen atom accumulating on the surface. Vacuum system is powerful enough to ignore resorption at the outlet (in condition (26)). A more accurate model of "surface-bulk'' is

$$k^+(T)c_{0,H}\left[1 - q_{o,H}q_{\max}^{-1}\right] - k^-(T)\left[1 - c_{0,H}c_{\max}^{-1}\right] = \mp D(T)\partial_z c|_{0,H}.$$

Both hydrogen flux from the bulk to the surface and flux caused by hydrogen dissolution in the bulk are proportional to concentrations with regard to "vacant spac". However, we obtain the condition of relatively fast solubility $c_{0,H} = gq_{0,H}$, $g = k^-/k^+$ when diffusion is much slower (not at low temperatures) and concentrations are small. If the surface is isotropic (i.e. meaning $E_{k^-} \approx E_{k^+}$), then the parameter g weakly depends on T. Surface and near-surface bulk concentrations proportionally "monitor" one another. Dynamic boundary conditions (25), (26) allow to take into account and estimate storage effect of hydrogen atoms on the surface. These conditions are agreed (in the classical context) with zero initial data $c(0,r,z) = 0$ (as $t \to +0$). However, it should be borne in mind that generally, $\partial_t q_0(0,r) = \mu sp \gg 1$ (depending on the material, the temperature and inlet pressure).

The model hierarchy is that we derive the boundary conditions (20), (21) from slight accumulation of $\partial_t q_{0,H}$ on the surface. Values of surface and bulk desorption coefficients (denoted by the same symbol and distinguished by the context) are assumed to be agreed: $b_{\text{surf}} = g^2 b_{\text{vol}}$ ($bq^2 = bc^2$, $c = gq$).

A. Algorithm of Numerical Solution

DOI: 10.5963/AMSA0302005

Counter-sweep method. Let us consider the calculation of the near-surface concentrations $\hat{c}_{i,0}$, $\hat{c}_{i,N_2}$, $i \le i_0$. To maintain the order of approximation to $O(\tau^2 + h_z^2)$, we use the scheme with weights

$$\frac{\hat{c}_{i,0} - c_{i,0}}{g\tau} = \sigma[\mu sp - b(\hat{c}_{i,0}g^{-1})^2 + D\partial_z\hat{c}_{i,0}] + (1-\sigma)[\mu sp - b(c_{i,0}g^{-1})^2 + D\partial_z c_{i,0}],$$

$$\frac{\hat{c}_{i,N_2} - c_{i,N_2}}{g\tau} = \sigma[-b(\hat{c}_{i,N_2}g^{-1})^2 - D\partial_z\hat{c}_{i,N_2}] + (1-\sigma)[-b(c_{i,N_2}g^{-1})^2 - D\partial_z c_{i,N_2}],$$

for conditions (1), (2) assuming $\sigma = 1/2$. Here τ is a step at time t; and derivatives $\partial_z c_{i,0}$, $\partial_z c_{i,N_2}$ are approximated expressions, similar to (22). As in the modification of the model for the bulk desorption (saving denotes $\mathbb{A}$, $\mathbb{B}$, $\widehat{\mathbb{B}}$, $\mathbb{G}$), finding of $\hat{c}_{i,0}$, $\hat{c}_{i,N_2}$ is reduced to solving the quadratic equations system:

$$\begin{cases} \dfrac{b}{g^2}\,\hat{c}_{i,0}^2 + \left(\dfrac{D\mathbb{A}}{2h_z} + \dfrac{2}{g\tau}\right)\hat{c}_{i,0} + \dfrac{D\mathbb{G}}{2h_z}\hat{c}_{i,N_2} + \dfrac{D\widehat{\mathbb{B}}}{2h_z} + C_1 = 0 \\ \dfrac{b}{g^2}\,\hat{c}_{i,N_2}^2 + \left(\dfrac{D\mathbb{A}}{2h_z} + \dfrac{2}{g\tau}\right)\hat{c}_{i,N_2} + \dfrac{D\mathbb{G}}{2h_z}\hat{c}_{i,0} + \dfrac{D\mathbb{B}}{2h_z} + C_2 = 0, \end{cases}$$

where $C_1 \equiv bg^{-2}c_{i,0}^2 - 2(g\tau)^{-1}c_{i,0} - D\partial_z c_{i,0} - 2\mu sp$, $C_2 \equiv bg^{-2}c_{i,N_2}^2 - 2(g\tau)^{-1}c_{i,N_2} + D\partial_z c_{i,N_2}$.

Iteration method. The scheme with the weighting coefficients ($\sigma = 1/2$, the order of approximation to $O(\tau^2 + h_z^2)$) is used for the boundary conditions (1), (2):

$$\frac{\hat{c}_{i,0} - \bar{c}_{i,0}}{0.5\tau g} = 0.5[\mu sp - b(\hat{c}_{i,0}g^{-1})^2 + D\partial_z\hat{c}_{i,0}] + 0.5[\mu sp - b(\bar{c}_{i,0}g^{-1})^2 + D\partial_z\bar{c}_{i,0}],$$

$$\frac{\hat{c}_{i,N_2} - \bar{c}_{i,N_2}}{0.5\tau g} = 0.5[-b(\hat{c}_{i,N_2}g^{-1})^2 - D\partial_z\hat{c}_{i,N_2}] + 0.5[-b(\bar{c}_{i,N_2}g^{-1})^2 - D\partial_z\bar{c}_{i,N_2}].$$

The boundary values $\hat{c}_{i,0}$, $\hat{c}_{i,N_2}$ $(i \le i_0)$ are determined as the positive roots of the quadratic equations

$$\frac{b}{g^2}\,\hat{c}_{i,0}^2 + \left(\frac{3D}{2h_z} + \frac{4}{g\tau}\right)\hat{c}_{i,0} + C_1 = 0,$$

$$\frac{b}{g^2}\,\hat{c}_{i,N_2}^2 + \left(\frac{3D}{2h_z} + \frac{4}{g\tau}\right)\hat{c}_{i,N_2} + C_2 = 0,$$

$$C_1 \equiv \frac{D}{2h_z}\,(\hat{c}_{i,2} - 4\hat{c}_{i,1}) + \frac{b}{g^2}\,\bar{c}_{i,0}^2 - \frac{4}{g\tau}\,\bar{c}_{i,0} - D\partial_z\bar{c}_{i,0} - 2\mu sp,$$

$$C_2 \equiv \frac{D}{2h_z}\,(\hat{c}_{i,N_2-2} - 4\hat{c}_{i,N_2-1}) + \frac{b}{g^2}\,\bar{c}_{i,N_2}^2 + D\partial_z\bar{c}_{i,N_2} - \frac{4}{g\tau}\,\bar{c}_{i,N_2}.$$

Values $\hat{c}_{i,\{1,2\}}$, $\hat{c}_{i,\{N_2-1,N_2-2\}}$ (in expressions, similar to (22)) are pre-calculated by an explicit difference scheme approximating diffusion Eq. (1). Tridiagonal system of linear algebraic equations is solved with the current approximate values $\hat{c}_{i,0}$, $\hat{c}_{i,N_2}$, using a sweep method, and new approximate values $\hat{c}_{i,\{1,2\}}$, $\hat{c}_{i,\{N_2-1,N_2-2\}}$ (and the other values $\hat{c}_{i,j}$, $j = 3, \dots, N_2 - 3$, $i = 0, \dots, i_0$) are determined. We solve the quadratic equations in $\hat{c}_{i,0}$, $\hat{c}_{i,N_2}$ again and repeat the calculation, until boundary values are stabilized (usually 2–3 iterations are enough). To find boundary concentrations $\hat{c}_{i,N_2}$ for $i > i_0$, we approximate (2) with the accuracy to $O(\tau^2 + h_z^2)$ and use sweep coefficients determined by direct sweep when condition (3) operates:

$$bg^{-2}\hat{c}_{i,N_2}^2 + [D(2h_z)^{-1}\mathbb{A} + 2(\tau g)^{-1}]\hat{c}_{i,N_2} + \mathbb{B} = 0,$$

$$\mathbb{A} \equiv 3 + \alpha_{i,N_2}\Delta, \quad \Delta \equiv \alpha_{i,N_2-1} - 4,$$

$$\mathbb{B} \equiv -2\bar{c}_{i,N_2}(\tau g)^{-1} + D(\beta_{i,N_2-1} + \beta_{i,N_2}\Delta)(2h_z)^{-1}.$$

Roots of the quadratic equation have different signs for small h_z, τ, physically, thus we select a positive root. Calculated approximation $c_z(t,r,H)$ in the model (1)–(5); concentration $c(t,r,H)$ for boundary conditions (23), (24) and surface concentration $q_H(t,r)$ for the model modification (25), (26) provide a way to approximately calculate the permeation flux $J(t)$.

B. Numerical Modelling Results

DOI: 10.5963/AMSA0302005

We may pass to the dimensionless problem, as it was done above. However, the introduction of an additional parameter g does not reduce the number of independent numeric hydrogen permeability characteristics. In addition, it becomes more difficult to "return" to regularities, as observed in a real experiment. Hence we illustrate the model using physical units of measurement, focusing on the influence of surface processes parameters on the output flux ("derivatives" J to b, g, s). The following value specifies transport parameter estimation

$$W = HD^{-1}b_{\text{vol}}\bar{c} = HD^{-1}g^{-2}b\bar{c} = H[Dg]^{-1}\sqrt{\mu spb} \quad (\bar{c} = g\sqrt{\mu spb^{-1}}, \rho_0 = 1).$$

General geometric values of parameters: $L = 1$ cm, $H = 1/3$ cm, $r_0 = 0.1$ cm were fixed for presented computing experiments (Fig. 13-16). It should be noted that, the flux decreases with increasing b, because desorption on the inlet surface predetermines hydrogen permeability to a greater extent (decreases the equilibrium level of concentration $\bar{c}$).

Interesting effect is visible on Fig. 16. Steady state establishment time t_* decreases monotonically as the diffusion coefficient D $(10^{-7}–10^{-5})$ increases. In this case, stabilized flux level J_* increases at first and then decreases, because hydrogen atoms come up to the lateral isolated surface faster, get "reflexed" and thus increase concentration, simultaneously decreasing gradient ($|\partial_z c|$) and diffusion flux.

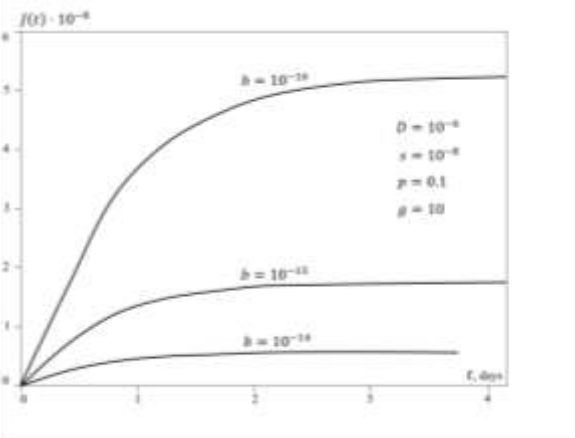

Fig. 13 Effect of a desorption coefficient

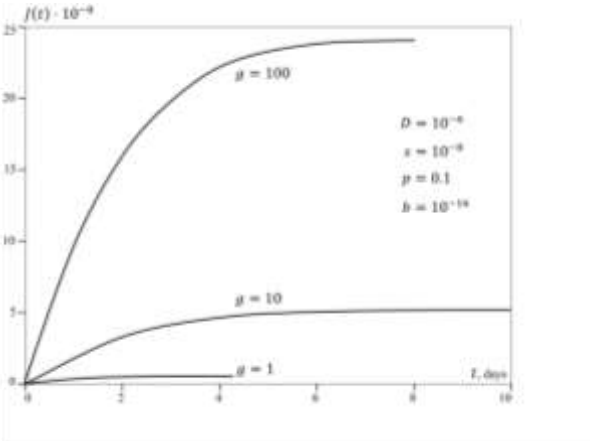

Fig. 14 Effect of a dissolution coefficient

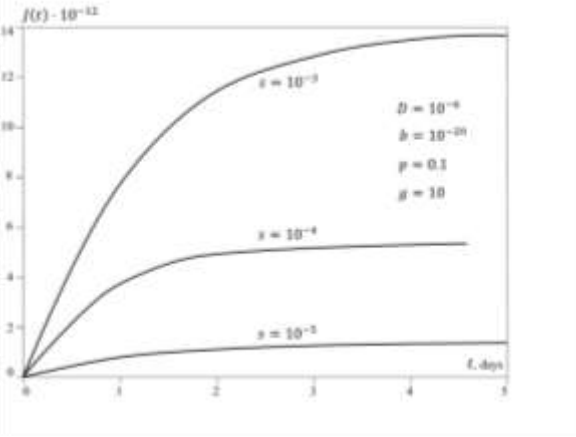

Fig. 15 Effect of an adhesion coefficient

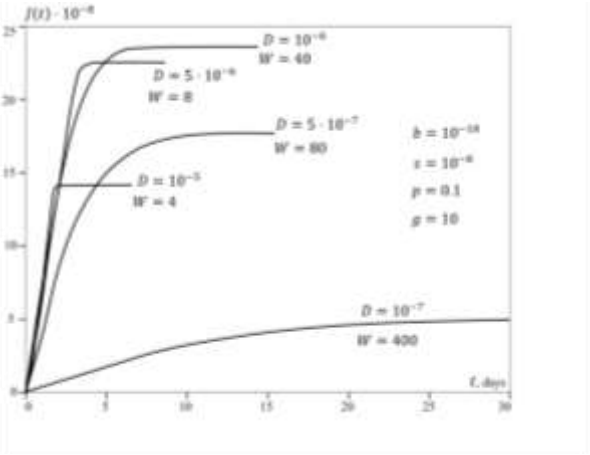

Fig. 16 Effect of a diffusion coefficient

VII. CONCLUSION

The paper presents the hydrogen permeability models of a cylindrical membrane made of a structural material in the presence of protective coating defect on the inlet surface. We take as the basis model the one with local equilibrium gaseous and dissolved under defect hydrogen when diffusion is the only limiting factor. Further hierarchy of the models consists in sequential accounting adsorption-desorption processes dynamics which results in non-linear and dynamic boundary conditions. Limit transition is valid: with reduction of hydrogen atoms accumulation on the surface, and with increase of desorption coefficient and inlet pressure, the model with nonlinear dynamic boundary conditions becomes a basic model.

Iterative computational algorithm to simulate outward hydrogen permeability flux is presented. The algorithm is based on implicit difference schemes. Qualitative regularities of the experimentally registered characteristics are identified (stationary flux level, stabilization and delay times) depending on the membrane geometric characteristics and on physical parameters

DOI: 10.5963/AMSA0302005

of hydrogen transfer into a constructional material. The influence of parameter variations on hydrogen permeability flux dynamics is illustrated.

The conditions under which the permeation flux is "insensitive" to boundary conditions are specified. Then the flux is proportional to the number of defects. This saves the cost of additional experiments. Interesting effect is detected: the time until steady state establishment decreases monotonically as the diffusion coefficient increases, but the stabilized flux level increases at first and then decreases. The described nonlinear effects should be taken into account when processing the experimental curves in order to identify the limiting factors and estimate the parameters. The results of numerical simulation provide a way to evaluate the distribution of the hydrogen concentration inside the membrane. These factors give information on the possible ways of treating the material (pre-training surface, various additives inside).

ACKNOWLEDGMENTS

The work was performed with the support of Basic Research Program, Branch of Mathematics, Russian Academy of Sciences. Numerical simulations were executed at the High-performance Data Treatment Centre in Karelian Research Centre of the Russian Academy of Sciences.

REFERENCES

[1] L.L. Kunin, A.M. Golovin, Yu.N. Surovoi, V.M. Hohrin, "Problems of metals degassing," Moscow: Nauka, 1972.

[2] J. Crank, *The mathematics of diffusion*, 2nd ed., Oxford: Clarendon Press, 1975.

[3] R.A. Varin, T. Czujko, Z.S. Wronski, "Nanomaterials for solid state hydrogen storage," New York: Springer, 2009.

[4] Eds. M. Ball, M. Wietschel, *The hydrogen economy*, Cambridge University Press, 2009.

[5] Ed. M. Hirscher, "Handbook of hydrogen storage: new materials for future energy storage," Germany: Wiley–VCH, 2010.

[6] A.A. Pisarev, I.V. Tsvetkov, E.D Marenkov, S.S. Yarko, "Hydrogen permeability through metals," Moscow: MEPhI, 2008.

[7] B. Zajec, "Hydrogen permeation barrier – recognition of defective barrier film from transient permeation rate," *Int. J. of Hydrogen Energy*, vol. 36, pp. 7353-7361, 2011.

[8] A.W. Warrick, P. Broadbridge, D.O. Lomen, "Approximations for diffusion from a disc source," *Appl. Math. Modelling*, vol. 16, pp. 155-161, 1992.

[9] L. Rajendran, M.V. Sangaranarayanan, "A two-point Pade approximation for the non-steady-state chronoamperometric current at ultramicrodisc electrodes," *J. of Electroanalytical Chem*, vol. 392, pp. 75-78, 1995.

[10] A.A. Samarskii, "The theory of difference schemes," New York: Marcel Dekker, Inc, 2001.

[11] G. Birkhoff, G.– C. Rota, "Ordinary differential equations," New York: John Wiley & Sons, 1989.

[12] N.N. Kalitkin, "Numerical methods," Moscow: Nauka, 1978.

[13] Yu.V. Zaika, "Identification of a hydrogen transfer model with dynamical boundary conditions," *Int. J. of Mathematics and Mathematical Sci.*, vol. 4, pp. 195-216, 2004.

[14] Yu.V. Zaika, E.P. Bormatova, "Parametric identification of a hydrogen permeability model by delay times and conjugate equations," *Int. J. of Hydrogen Energy*, vol. 36, pp. 1295-1305, 2011.

[15] I. Ali-Khan, K.J. Dietz, F.J. Waelbroeck, P. Wienhold, "The rate of hydrogen release out of clean metallic surfaces," *J. of Nuclear Materials*, vol. 76-77, pp. 337-343, 1978.

[16] A. Pisarev, "Hydrogen gas-driven permeation through the membrane with asymmetric surface conditions," *J. of Membrane Sci.*, vol. 335, pp. 51-57, 2009.

[17] Yu.V. Zaika, N.I. Rodchenkova, "Boundary-value problem with moving bounds and dynamic boundary conditions: diffusion peak of TDS-spectrum of dehydriding," Appl. Math. Modelling, vol. 33, pp. 3776-3791, 2009.

Yury V. Zaika was born in 1960, in USSR. Positions: Head of the Laboratory of Natural-Technical System Modelling, Institute of Applied Mathematical Research; Professor of Dept. of Applied Mathematics and Cybernetics, Petrozavodsk State University. Academic degrees: PhD (mathematical cybernetics), Leningrad (St. Petersburg) State University, 1985; Doctor (DSc) of Physics and Mathematics (mathematical modelling), St. Petersburg Institute for Informatics and Automation of RAS, 1998. Academic status: Professor (2002). Major research trends: Mathematical Theory of Control; Inverse Problems of Mathematical Physics; Mathematical Modelling of Hydrogen Interaction with Solids.

Ekaterina K. Kostikova was born in 1982, in Petrozavodsk, Russia. Positions: Researcher in the Laboratory of Natural-Technical System Modelling, Institute of Applied Mathematical Research (Petrozavodsk, Russia); Lecturer of Dept. of Applied Mathematics and Cybernetics, Petrozavodsk State University. Academic degree: Cand. (PhD) of Physics and Mathematics (2012, Petrozavodsk State University). Scientific specialty is mathematical modelling, numerical methods and software complexes.

2000-2006: Student of the Faculty of Mathematics, Petrozavodsk State University. 2006-2012: PhD Student of Institute of Applied Mathematical Research, Karelian Research Centre of the Russian Academy of Sciences. Major research trends: Mathematical Modelling of Physical Processes; Boundary-Value Problems of Mathematical Physics; Numerical Methods.

DOI: 10.5963/AMSA0302005